Hydrogeomorphic and biotic drivers of instream wood differ across sub-basins of the Columbia River Basin, USA

Nate Hough-Snee[1,2,*], Alan Kasprak[1], Rebecca K. Rossi[1], Nick Bouwes[1,3], Brett B. Roper[1,4], Joseph M. Wheaton[1,2]

[1]Utah State University, Department of Watershed Sciences
5210 Old Main Hill
Logan, UT 84322-5210

[2]Utah State University, Ecology Center
5205 Old Main Hill
Logan, UT 84322-5205

[3]Eco Logical Research, Inc., P.O. Box 706, Providence, UT, 84332, USA

[4]USDA Forest Service Forest Sciences Laboratory
860 N 1200 E
Logan, UT 84321

*Corresponding author: nate@natehough-snee.org; 1.435.535.5085

Keywords: Large woody debris, ecogeomorphology, wood transport, riparian vegetation, stream assessment, aquatic habitat, Columbia Habitat Monitoring Program, riparian ecology

Short title: Columbia Basin instream wood

Abstract

Instream wood promotes habitat heterogeneity through its influence on flow hydraulics and channel geomorphology. Within the Columbia River Basin, USA, wood is vital for the creation and maintenance of habitat for threatened salmonids. However, our understanding of the relative roles of the climatic, geomorphic, and ecological processes that source wood to streams is limited, and making it difficult to identify baseline predictions of instream wood and create targets for stream restoration. Here we investigate how instream wood frequency and volume differ between seven sub-basins of the Columbia River Basin and what processes shape these differences within these sub-basins. We collected data on wood volume and frequency, discharge and stream power, and riparian and watershed forest structure for use in modeling wood volume and frequency. Using random forest models, we found that mean annual precipitation, riparian tree cover, and the individual watershed were the most important predictors of wood volume and frequency. Within sub-basins, we used linear models, finding that some basins had unique predictors of wood. Discharge, watershed area or precipitation often combined with forest cover, riparian conifer and/or large tree cover in models of instream large wood volume and frequency. In many sub-basins, models showed at least one hydrologic variable, indicative of transport capacity and one ecological variable, indicative of the reach or upstream watershed's ability to grow measurable instream wood. We conclude that basin-specific models yield important insights into the hydrologic and ecological processes that influence wood loads, creating tractable hypotheses for building predictive models of instream wood.

Introduction

Wood serves as a keystone geomorphic control in low-order streams, driving stream hydraulics that influence sediment erosion and deposition (Malanson and Butler 1990; Gurnell *et al.* 2002; May and Gresswell 2003), channel planform (Polvi and Wohl 2013) and habitat heterogeneity (Johnson *et al.* 2005). Where wood is found in streams, it creates heterogeneity in the flow field (Manners *et al.* 2007), leading to hydraulic diversity that creates and maintains diverse assemblages of geomorphic units (Beschta 1979; Thompson 1995; Assani and Petit 1995; Abbe and Montgomery 1996). The diversity of geomorphic units created by instream wood provide habitat for numerous aquatic biota (Fausch and Northcote 1992), and as such, instream wood is commonly studied in the context of fish habitat (Ralph *et al.* 1994; Beechie and Sibley 1997; Cederholm *et al.* 1997). The presence of instream wood buffers channels against large-scale degradation during high flows (Fausch and Northcote 1992; Faustini and Jones 2003). At the same time, instream wood facilitates sediment deposition that provides colonization sites for seedling recruitment, creating a positive feedback that promotes future wood growth and recruitment (Gurnell *et al.* 1995).

Three important broad-scale factors that shape instream wood loads are (1) the potential of watersheds and riparian areas to grow forest vegetation that can be contributed to the channel as wood (Hough-Snee *et al.* 2014a), (2) mechanisms that contribute wood to channels and floodplains (Martin and Benda 2001), and (3) streamflow and channel forms that allow wood to be transported and deposited within a stream network (Braudrick *et al.* 1997). The environmental capacity of a landscape to grow large trees (e.g. climate, land-use) intersects with a given hillslope or floodplain's potential to contribute wood to channels, and a stream reach's propensity for wood transport or retention (*sensu* (Hough-Snee *et al.* 2014a). These ecological and hydrogeomorphic factors' relative importance in shaping instream wood dynamics may vary markedly across environmental gradients associated with topography and climate. For example, large basins show climatic (e.g. temperature, precipitation) and disturbance (e.g. logging, grazing, roads) gradients that shape forest composition, structure, and regeneration from headwaters to valley bottoms (Sarr *et al.* 2011; Hough-Snee *et al.* 2014b). These gradients effectively limit the sources of wood that can eventually be grown and recruited to streams.

The pathways by which wood is recruited and retained in streams are numerous (Benda *et al.*, 2003). Direct tree fall into channels is an important mechanism by which local sources of wood reach the channel (Bragg and Kershner 2004). Lateral migration of streams into tree-covered banks and mass wasting of forested hillslopes are also vital wood recruitment mechanisms (Kasprak *et al.* 2012). Wildfire and insect outbreaks can accelerate tree mortality and promote tree fall into channels, as can ice and wind storms (Bragg 2000). Once in the channel, wood is transported downstream by the force of the flow (Braudrick *et al.* 1997). In many cases, high flow events with sufficient stream power transport large wood through stream networks (Braudrick and Grant 2000; Martin and Benda 2001). Aside from flow stage, several factors affect the relative mobility of particular wood pieces. The presence of large, 'keystone' pieces can act to trap smaller pieces, thus creating jams, increasing overall wood retention and lowering transport distances (Montgomery *et al.* 2003). Accordingly, the length of a wood piece compared to the bankfull width of a channel, or the structural elements of a wood piece (e.g. root bundle, branched canopy crown), may indicate its propensity for mobility during a given flow (Bilby and Ward 1989; Polvi *et al.* 2011). The potential for particular flows to do work is often approximated as stream power, and can influence wood retention, as pieces are typically removed from high-gradient reaches and deposited in lower-gradient areas (Magilligan *et al.* 2008; Fisher *et al.* 2010).

When considering geomorphically and hydraulically diverse stream channels that provide habitat for aquatic biota, the prevailing view of wood has been "*more is better*" (Cederholm *et al.* 1997; Floyd *et al.* 2009). In turn, there is a strong demand to understand the relationships between processes that result in *more* wood in streams, both within and between basins, along with the mechanisms by which wood is retained or transported at the reach scale. This balance between wood growth, recruitment, and retention (Gurnell *et al.* 1995) remains largely unexplored across large landscapes, leaving watershed and aquatic habitat managers without clear guidance on the specific factor(s) that may limit wood volume or frequency at a given reach within a watershed.

To make inferences about how wood loads and controls differ across landscapes, we analyze instream wood volume and frequency data from seven sub-basins of the Columbia River Basin, USA (Figure 1), each of which is considered ecologically valuable due to local populations of threatened or endangered native salmonids (Nehlsen 1997). In each sub-basin, we seek to understand the hydrogeomorphic and ecological processes that lead to wood recruitment and retention in monitored stream reaches, using field-based monitoring data and freely-available remote sensing data describing riparian vegetation, climate, and geomorphic attributes of stream reaches. To achieve this, we first seek to (1) quantify the volume and frequency of instream wood in reaches across these sub basins, and subsequently (2) determine which riparian, geomorphic, and hydrologic attributes are most strongly correlated to instream wood loads both within and between individual sub basins.

Methods

Site Description

The Columbia River Basin (CRB) spans across southern British Columbia and Alberta, Canada to the U.S. states of Oregon, Washington, Idaho, and portions of Montana, Nevada and Utah (Figure 1). The Columbia River is one such basin where instream wood, and the ecological, hydrologic, and geomorphic factors that drive it, vary widely among and within tributary sub-basins. Accordingly, wadeable streams (small streams often less than 5th order that can be sampled on the ground without watercraft; (USEPA 2006) are currently monitored to assess habitat conditions for anadromous salmonids (Bragg and Kershner 2004; CHaMP 2013). In these small streams, wood often exerts strong effects on the formation of geomorphic units (Gurnell *et al.* 2002; Wohl and Beckman 2014), and is commonly monitored to evaluate baseline stream conditions and identify relationships between wood and habitat attributes (Hough-Snee *et al.* 2014a). Within the CRB there are several targeted sub-basins wherein wadeable streams are regularly monitored as a part of the Columbia Habitat Monitoring Program (CHaMP), an ongoing salmonid habitat status and trend monitoring program (CHaMP 2013). Here we used status data collected in 2011 and 2012 in seven sub-basins: the Entiat, Wenatchee, and Tucannon Rivers in Washington State, the John Day and upper Grande Ronde Rivers in Oregon, and the Lemhi and South Fork Salmon Rivers in Idaho. These basins were selected from within the larger CHaMP study region based on their importance to regional aquatic habitat conservation and physiographic and climatic diversity (Tables 1 and 2).

Stream, Large Wood, and Riparian Data

In situ stream physical and hydrogeomorphic data were collected as a part of CHaMP's stream habitat monitoring framework (CHaMP 2013). Each reach was surveyed to create a digital elevation model (DEM; 0.1 m cell resolution), from which surface water gradient, channel sinuosity, and channel bankfull width were calculated. At each reach, ten 10 m^2 riparian vegetation plots were sampled for canopy cover of woody species, conifer species, and large trees (diameter at breast height >30cm). The percent of woody species, conifer species and large tree cover at each reach were calculated by averaging the cover from within plots at that reach. Base flow discharge was measured at each reach using standard cross-section methods (Peck *et al.* 2002). Wood was sampled concurrently with riparian vegetation and stream metrics using the methods outlined in (CHaMP 2014). Under this protocol, instream wood was identified as any unrooted wood larger than one meter in length and greater than 10cm in diameter overhanging the bankfull channel. Each of the first ten wood pieces and thereafter every tenth piece's length and diameter were measured while diameter and length were estimated for the nine pieces between measurements. From these measurements, a total wood frequency (count: pieces/reach) and volume (m^3/reach) were estimated at each reach. Because CHaMP-monitored reaches' length vary (reach length = 20-times bankfull width), both frequency and volume were scaled to a standardized length, in this study, pieces km^{-1} and m^3 km^{-1}.

Watershed Climate, Vegetation, and Stream Power

We used freely available GIS data to assemble attributes of each watershed environment. We used USGS 10 m resolution National Elevation Dataset DEMs to derive average catchment area above each reach, calculating vegetation and climate for each catchment. We paired DEMs with PRISM climate data (PRISM Climate Group, 2012) to calculate the 30-year mean annual precipitation between 1970 and 2000 in each catchment. Using LANDFIRE data, we calculated the proportion of each catchment that was forested under any of LANDFIRE's forest cover classes. We also buffered each reach within a 30-meter area around the sampled reach and calculated forest cover from LANDFIRE cover classes.

We used USGS regional curves (Table S1) to calculate discharge at each reach under two-year (Q_2), 10-year (Q_{10}), and 25-year (Q_{25}) flood-recurrence intervals. This discharge was converted to unit stream power (ω) using Equation 1:

$$\omega = \frac{\gamma Q_{RI} S}{b} \qquad (1)$$

ω= *γQRISb*

Where γ is the specific weight of water, Q_{RI} is the discharge at the recurrence interval of interest, S is the reach-averaged channel gradient, and b is the field-surveyed reach-averaged bankfull width. Because both gradient and bankfull width are incorporated into unit stream power calculations, these terms were not used as predictors within statistical models.

Statistical Analysis

Our analysis proceeded in two stages, assessing the factors that corresponded to instream wood within all sub-basins, and then identifying differences in wood volume and frequency within individual sub-basins. We used random forest (RF) models to identify relationships between

PeerJ PrePrints | https://dx.doi.org/10.7287/peerj.preprints.1256v1 | CC-BY 4.0 Open Access | rec: 21 Jul 2015, publ: 21 Jul 2015

hydrogeomorphic and ecological attributes that influence instream wood accumulation and movement within all seven sub-basins. Random forest models included three field-measured forest cover metrics: percent large tree, riparian woody vegetation, and riparian conifer cover, and two remotely sensed forest cover metrics: percent reach forest cover and percent catchment forest cover. Seven hydrogeomorphic variables were also included in the models: site sinuosity, unit stream power calculated for Q_2, Q_{10} and Q_{25} discharge, base flow discharge, mean annual precipitation, and watershed area. We included a categorical term for each watershed to provide evidence for different wood loads between sub-basins. We used all variables to model wood volume and frequency for all 300 reaches. Volume and frequency were log+1 transformed prior to all analyses due to dispersion within each variable. The RF approach was reasonable for modeling wood loads across all reaches and with all predictors as RFs make no assumptions about the distribution of error terms or relationships between variables (Cutler *et al.* 2007). Random forests are an ensemble learning method that grows “forests” from individual regression trees. Our models used 9,999 trees grown by fitting as many as four predictor variables at each node. All RF models were implemented in the randomForest package (Liaw and Wiener 2002) in the R statistical environment (R Core Team 2014).

To visualize reaches’ and sub-basins’ relative similarity, we performed non-metric multidimensional scaling (NMDS) on a matrix of hydrogeomorphic and forest cover variables, excluding instream wood frequency and volume. Variables were log+1 transformed prior to analysis and inter-reach distances were calculated using Bray-Curtis distance. To visualize environmental gradients across sub-basins, we fit each forest cover, hydrogeomorphic, and wood metric to the ordination space using multiple regression (metaMDs and envfit functions in R).

Following interpretation of RF and NMDS results, we tested the null hypothesis that wood loads did not differ between basins using PERMANOVA (Anderson 2005) and Bonferroni corrected, permutation-based t-tests (999 permutations; RVAideMemoire package in R; Piegay 2015). We hypothesized that wood loads differed across many, if not all of the sub-basins, as each sub-basin may have a different capacity for growing and transporting wood based on climate, hydrology and reach setting.

We built ordinary least squares linear regression models of wood volume and frequency within each sub-basin to see how wood predictors differed between sub-basins. The same variables were used in regression modeling of each sub-basin as were used in the global RF model, with minor changes. Prior to sub-basin analyses we examined relationships between each predictor variable within that sub-basin. If correlations between any pair of variables were equal to or greater than 0.60, one of the variables was removed. Q_2, Q_{10} and Q_{25} unit stream power were highly correlated in all sub-basins, so only Q_{25} unit stream power was retained for individual sub-basin models. Of the three estimates Q_{25} was selected because of the importance of relatively large, rare flood events in mobilizing and transporting wood. Models were built for each sub-basin with all possible uncorrelated variables and then iteratively selected by comparing models' Bayesian Information Criterion (BIC; regsubsets function; leaps package in R; (Miller 2009).

Results

Wood loads across the Columbia River Basin

Both wood frequency and volume varied among and within the seven sub-basins (Figure 3). Across the CRB wood frequency ranged from 0 to 2117.0 pieces km^{-1} while volume ranged from

0 to 539 m^3 km^{-1}. Large wood volume (PERMANOVA F = 5.1; *P* =0.001) and frequency (PERMANOVA F = 5.4; *P* =0.001) differed significantly between sub-basins. At the sub-basin scale, average wood frequency ranged from 142.1 ± 17.7 pieces km^{-1} (John Day) to more than 358.7 ± 72.3 pieces km^{-1} (South Fork Salmon). Pairwise comparisons showed that wood frequency was highest in the South Fork Salmon, Tucannon, Grande Ronde, and Entiat, and lowest in the Wenatchee, Lemhi, and John Day (Figure 3). Wood volume was lowest in the Lemhi (22.1 ± 4.2 m^3 km^{-1}) and greatest in the South Fork Salmon (190.3 ± 66.6 m^3 km^{-1}). Wood volume in the Tucannon, Grande Ronde, Wenatchee, Entiat and John Day did not significantly differ.

Random forest models showed that mean annual precipitation, riparian large tree cover and individual watershed were the three most important predictors of wood volume and wood frequency at reaches within all sub-basins (Figure 4, S1, S2). Watershed area was the fourth strongest predictor of wood frequency while catchment- and reach-scale forest cover were the fourth and fifth strongest predictor of wood volume. Sinuosity and measures of streamflow and stream power were relatively weak predictors of both wood volume and frequency (Figure 4). Overall, wood frequency/volume increased with precipitation and riparian large tree cover and decreased with watershed area. The final RF models explained 43.5% of the variance in volume and 42.0% of the variance in frequency.

The final NMDS solution of hydrogeomorphic and forest variables (stress = 0.10) showed strong environmental gradients within and between sub-basins. Q_{10} and Q_{25} unit stream power (R^2 = 0.69; R^2 = 0.69), reach forest cover (R^2 = 0.63), Q_2 unit stream power (R^2 = 0.58), and riparian

PeerJ PrePrints | https://dx.doi.org/10.7287/peerj.preprints.1256v1 | CC-BY 4.0 Open Access | rec: 21 Jul 2015, publ: 21 Jul 2015

conifer cover ($R^2 = 0.54$) were most strongly correlated to the final NMDS solution of all environmental attributes (Figure 5). Watershed area, unit stream power, and baseflow discharge gradients were strongest across the second NMDS axis while gradients of precipitation, large tree, riparian woody vegetation, and catchment forest cover were strongest across the first NMDS axis. In stream wood volume ($R^2 = 0.06$) and frequency ($R^2 = 0.09$) were only weakly correlated to the NMDS solution (Figure 5; Table S3). Most illustrative within the NMDS ordination were the inverse correlations between wood volume and frequency and watershed area and baseflow discharge. Positive correlations between wood volume and frequency and riparian conifer cover, reach and catchment forest cover were also evident. Individual sub-basins were distributed across the precipitation, riparian woody and large tree cover, and sinuosity gradients that corresponded to NMDS axis 1 and watershed area, unit stream power, and baseflow discharge gradients across NMDS axis 2.

Drivers of wood frequency and volume between sub-basins

Within the Entiat, regression models showed that precipitation and watershed area were the most consistent predictors of wood volume while reach forest cover and riparian conifer cover were consistent predictors of wood frequency. None of the candidate models for volume or frequency within the Entiat had strong predictive power ($R^2 \leq 0.12$). Models for the John Day, which had shown sites distributed across forest cover gradients (Figure 5), showed that reach forest cover and large tree cover were predictors in all models and five of six models respectively. Within the John Day, models for wood volume had stronger predictive power (all $R^2 > 0.55$) than models for wood frequency (all $R^2 \leq 0.45$). These models had some of the highest predictive power of all sub-basin models. Catchment forest cover was positively correlated to wood volume and frequency in all models within the Lemhi. Watershed area was positively correlated to wood volume and frequency in all volume models and two of the top three frequency models. Q_{25} unit stream power was positively correlated to wood volume and frequency in one of the final models for each while large tree cover had a positive effect in one volume model.

Baseflow discharge had a negative effect on all wood volume and frequency models within the South Fork Salmon while riparian woody cover also had a negative effect in two of three models for wood volume and frequency. Reach forest cover had positive effects in one model each for volume and frequency, while large tree cover had a positive effect in one volume model. Catchment forest cover had a positive effect on wood volume and site sinuosity had a positive effect on wood frequency throughout the Tucannon sub-basin models. Q_{25} unit stream power was positively correlated to large wood frequency in two models while large tree cover was negatively correlated to large wood volume.

Within the Upper Grande Ronde, watershed area was negatively related to wood volume and frequency in all models. Catchment forest cover and riparian conifer cover were positively related to wood frequency while baseflow and reach forest cover were positively related to wood volume. The Wenatchee sub-basin showed that watershed area and baseflow discharge were negatively related to wood volume and frequency while precipitation and Q_{25} unit stream power were positively related to wood volume. Riparian conifer cover was positively related to wood volume in all models while riparian woody cover was positively related to wood frequency in all models.

Discussion and Conclusions

Setting baseline expectations for wood loading at the reach scale requires identifying and differentiating the processes that recruit wood within geographically distinct watersheds and the processes that export wood from a given reach. In the CRB, we found that instream wood volume and frequency are distinctly different between seven sub-basins. The larger CRB-wide model showed that strong gradients in precipitation, large tree cover, and reach and catchment forest cover shaped instream wood volume and frequency. These gradients corresponded to differences in both wood volume and frequency, and their explanatory hydrologic and ecological processes, in individual sub-basins. While the direct and indirect effects of climate, geomorphic setting, disturbance, and riparian vegetation on instream wood have been previously shown across the CRB (Hough-Snee *et al.* 2014a), here we show that while such large-scale models are useful in explaining general concepts in riparian ecology, predictive models of wood loads may be similarly informative when focused on specific sub-basins.

We anticipated that an increased capacity of catchments and riparian zones to grow wood would increase wood loads within the larger CRB and across study sub-basins. This expectation was generally met, but with subtle differences in direction and size of the effects of riparian forest cover. In the Entiat, Tucannon, South Fork Salmon sub-basins, either riparian conifer, large tree, or woody cover were negatively related to wood volume or frequency. In the random forest models for the CRB (Figures S1, S2), there were distinct drops in volume and frequency as riparian woody cover and coniferous cover initially increased. In particular, riparian coniferous cover caused an initial decline and then sharp increase in wood frequency before leveling out as conifer cover reached close to 20% (Figure S2). This observation and the other basin-specific wood-vegetation relationships may be related to the particular riparian landform surfaces where riparian vegetation was measured. For example, much of the Tucannon is relatively confined due to channel incision, and may be unable to access floodplain vegetation, where large trees are increasingly distant from the active channel, during all but the largest floods. Additionally, as flooding and successional processes continuously shape riparian forests, it is possible that floodplains may be covered in woody vegetation, but no individual tree species large enough to contribute to the channel (e.g. riparian willow forest or mesic shrublands) as measurable instream wood. These results indicate that in the Tucannon, wood must be added or transported from far upstream.

We anticipated that unit stream power would influence the volume and frequency of wood within both basins and at individual stream reaches as wood may be preferentially mobilized through, and exported from, reaches with greater stream power (Magilligan *et al.* 2008; Fisher *et al.* 2010). However, we found that unit stream power had relatively little predictive power in terms of instream wood frequency and volume at both the basin (Figure 4) and reach scale (Table 3). Only three of the six sampled sub-basins demonstrated significant, yet weak, correlations between wood frequency or volume and Q_{25} unit stream power (Table 3). We suggest that the low relative importance of unit stream power is an artifact of both basin-scale variability in wood transport capacity, and the potential for channels to trap large volumes of wood at discrete storage sites (e.g. jams). In the former case, channel networks do not function simply as homogeneous conduits for wood or sediment transport, but rather are marked by discrete, along-profile areas of variability in channel gradient or dimensions that manifest as localized zones of increased or decreased transport competence. Examples of such areas include beaver ponds, bedrock gorges, mainstem lakes, and reach-scale variations in valley width, to name just a few (Montgomery 1999; Walter and Merritts 2008; Polvi and Wohl 2013).

These discrete areas of increased or decreased transport competence for wood may occur at numerous locations along a stream profile, and it is impossible to capture all of them using a reach-scale sampling campaign such as the site-specific monitoring data used here. As such, the accumulation or evacuation of wood from discrete zones along a stream may result in wood volume or frequency estimates in downstream reaches that vary markedly from those predicted using stream power calculations alone. In addition, wood jams that occur at even finer scales (e.g. < 0.1 km) are typically marked by the presence of large, 'key' or 'anchor' pieces that subsequently rack smaller pieces tightly in place (Montgomery *et al.* 2003). Wood jams are quite stable, often persisting for decades to centuries, remaining in place despite the passage of large floods (Gregory 1991; Macdonald *et al.* 1995; Braudrick *et al.* 1997). Typical discharges that may drive the mobility of individual pieces of wood may not be sufficient to transport large quantities of wood that are often stored in stable jams, thus rendering stream power a poor predictor of wood retention or export from a reach.

The relationships between hydrologic variability and watershed and riparian ecosystem structure and large wood may not be well explained by the remote sensing and rapid assessment-based riparian vegetation data used here. Because the CHaMP protocols for riparian woody, conifer and large tree cover are based on small (10m x 10m) plots placed adjacent to the channel, we used riparian buffer and catchment-scale forest cover as surrogates for upland trees that may be contributed to the channel. While this provides a comprehensive estimate of forest coverage locally, and within the upstream area, it does not provide any spatial structure data as to where large trees are, or which species make up the large trees. To inform both riparian forest community ecology, and elucidate the drivers of wood-mediated ecosystem services like habitat and instream wood, we suggest monitoring riparian forests in a spatially explicit way that allows for stand modeling across riparian areas and floodplains. By specifically linking tree size to stream size, flow and geomorphic evolution, more informed hypotheses can be developed about how riparian forests shape instream wood loads and dynamics over time.

In stream management and restoration, a popular sentiment is that streams which contain more wood also contain higher quality aquatic habitat (Gurnell *et al.* 1995). However, we caution that, given the significant differences in background wood loads within sub-basins of the CRB, natural increases in wood may not be uniform, or even possible. These sub-basins, all of which are of high conservation interest due to the presence of threatened salmonids, will likely require instream wood additions to meet habitat restoration goals. This may be particularly true where processes governing forest growth and succession and/or wood recruitment and transport are limited. At the CRB scale, we found that climatic variables (e.g. precipitation) that dictate the growth of large riparian trees, commonly influence the volume and frequency of instream wood (Figure 4). Basins that span large climatic gradients are unlikely to exhibit uniform wood loading given the differing potential supply of wood to channels. Differences in wood supply and recruitment may also result from valley-scale variability in channel planform and hillslope characteristics that provide pathways for wood recruitment, leading to stream reaches or entire basins being intrinsically wood-limited (Kasprak *et al.*, 2012).

Large-scale disturbance, either natural or anthropogenic, provide likely mechanisms to recruit wood to channels. For example, the extent and severity of wildfire, along with the time elapsed since burning, may all play a role in increasing rates of tree fall and subsequent delivery to streams (Bragg 2000; Figure 2). Alternatively, human disturbance, including wood removal from streams (Wohl 2014) riparian grazing (Hough-Snee *et al.* 2013), or road development that facilitates logging and other land uses that reduce watershed forest cover (Bilby and Ward 1991; Meredith *et al.* 2014) may alter wood delivery rates to streams. These disturbance mechanisms occur heterogeneously throughout our study region (Hough-Snee *et al.* 2014a). Historically poor documentation of wood removal, and riparian logging and grazing may preclude accurately characterizing historic instream wood estimates. Similarly, contemporary, undisturbed reference sites are often high in watersheds, far from valley bottom streams most in need of restoration. This spatial disconnect may make it difficult to decouple human disturbance from hydrogeomorphic processes that differ naturally across process domains (Montgomery 1999). Because CHaMP data do not include such disturbance or historic wood removal metrics, we do not quantify their influence on instream wood loads here. Future research into the specific mechanisms that result in heterogeneous wood loading between basins would benefit from the incorporation of disturbance-related data, including such metrics as wood removal, wildfire, grazing, urbanization, or road construction.

Acknowledgements

Support was provided by grants from the Bonneville Power Administration to Eco Logical Research (BPA Project Number: 2003-017), Inc. and subsequent grants from ELR to Utah State University (USU Award ID: 100652). NH-S was supported in part by STAR Fellowship

Assistance Agreement no. 91768201 – 0 awarded by the U.S. Environmental Protection Agency (EPA). This research has not been formally reviewed by the EPA, NOAA, USFS nor BPA and the views expressed here are solely those of the authors. The EPA, NOAA, USFS, and BPA do not endorse any products or commercial services mentioned in this publication. We thank landowners for access, and CHaMP crews and partner organizations for data collection. We thank Reid Camp, Dan Hamill, Martha Jensen, Wally MacFarlane, and Peter McHugh for helpful feedback on manuscript drafts and Robert Williams for facilitating writing. The authors declare no conflict of interests. NH-S, NB, JMW, and BBR conceptualized the project, NH-S performed analyses, NH-S and RKR created figures and tables. All authors wrote the manuscript. NB, BBR and JMW made equal contributions and are listed alphabetically as authors.

References

Abbe TB, Montgomery DR. 1996. Large woody debris jams, channel hydraulics and habitat formation in large rivers. *Regulated Rivers: Research & Management* **12**: 201–221.

Anderson MJ. 2005. Permutational multivariate analysis of variance.

Assani AA, Petit F. 1995. Log-jam effects on bed-load mobility from experiments conducted in a small gravel-bed forest ditch. *Catena* **25**: 117–126.

Beechie TJ, Sibley TH. 1997. Relationships between Channel Characteristics, Woody Debris, and Fish Habitat in Northwestern Washington Streams. *Transactions of the American Fisheries Society* **126**: 217–229.

Beschta RL. 1979. Debris removal and its effects on sedimentation in an Oregon Coast Range stream. *Northwest Science* **53**: 71–77.

Bilby RE, Ward JW. 1989. Changes in Characteristics and Function of Woody Debris with Increasing Size of Streams in Western Washington. *Transactions of the American Fisheries Society* **118**: 368–378.

Bilby RE, Ward JW. 1991. Characteristics and function of large woody debris in streams draining old-growth, clear-cut, and second-growth forests in southwestern Washington. *Canadian Journal of Fisheries and Aquatic Sciences* **48**: 2499–2508.

Bragg DC. 2000. SImulating catastrophic and individualistic large woody debris recruitment for a small riparian system. *Ecology* **81**: 1383–1394.

Bragg DC, Kershner JL. 2004. Sensitivity of a riparian large woody debris recruitment model to the number of contributing banks and tree fall pattern. *Western Journal of Applied Forestry* **19***:* 117–122.

Braudrick CA, Grant GE. 2000. When do logs move in rivers? *Water Resources Research* **36***:* 571–583.

Braudrick CA, Grant GE, Ishikawa Y, Ikeda H. 1997. Dynamics of Wood Transport in Streams*:* A Flume Experiment. *Earth Surface Processes and Landforms* **22***:* 669–683.

Cederholm CJ, Bilby RE, Bisson PA, Bumstead TW, Fransen BR, Scarlett WJ, Ward JW. 1997. Response of Juvenile Coho Salmon and Steelhead to Placement of Large Woody Debris in a Coastal Washington Stream. *North American Journal of Fisheries Management* **17***:* 947–963.

CHaMP. 2013. The Columbia Habitat Monitoring Program*:* 2012 Second Year Lessons Learned Project Synthesis Report 2011-006. Bonneville Power Administration, Portland, OR

CHaMP. 2014. Scientific Protocol for Salmonid Habitat Surveys within the Columbia Habitat Monitoring Program. Portland, OR

Cutler DR, Edwards TC, Beard KH, Cutler A, Hess KT, Gibson J, Lawler JJ. 2007. Random forests for classification in ecology. *Ecology* **88***:* 2783–2792.

Fausch KD, Northcote TG. 1992. Large Woody Debris and Salmonid Habitat in a Small Coastal British Columbia Stream. *Canadian Journal of Fisheries and Aquatic Sciences* **49***:* 682–693.

Faustini JM, Jones JA. 2003. Influence of large woody debris on channel morphology and dynamics in steep, boulder-rich mountain streams, western Cascades, Oregon. *Geomorphology* **51***:* 187–205.

Fisher GB, Magilligan FJ, Kaste JM, Nislow KH. 2010. Constraining the timescales of sediment sequestration associated with large woody debris using cosmogenic ^{7}Be. *Journal of Geophysical Research*. **115**:F1

Floyd TA, MacInnis C, Taylor BR. 2009. Effects of artificial woody structures on Atlantic salmon habitat and populations in a Nova Scotia stream. *River Research and Applications* **25***:* 272–282.

Gregory S. 1991. Spatial and temporal patterns of woody debris retention and transport. *Bulletin of the North American Benthological Society* **8**: 75.

Gurnell AM, Gregory KJ, Petts GE. 1995. The role of coarse woody debris in forest aquatic habitats*:* Implications for management. *Aquatic Conservation: Marine and Freshwater Ecosystems* **5**: 143–166.

Gurnell AM, Piegay H, Swanson FJ, Gregory SV. 2002. Large wood and fluvial processes. *Freshwater Biology* **47***:* 601–619.

Hough-Snee N, Kasprak A, Roper BB, Meredith CS. 2014a. Direct and indirect drivers of instream wood in the interior Pacific Northwest, USA*:* decoupling climate, vegetation, disturbance, and geomorphic setting. *Riparian Ecology and Conservation* **2***:* 14–34.

Hough-Snee N, Roper BB, Wheaton JM, Budy P, Lokteff RL. 2013. Riparian vegetation communities change rapidly following passive restoration at a northern Utah stream. *Ecological Engineering* **58***:* 371–377.

Hough-Snee N, Roper BB, Wheaton JM, Lokteff RL. 2014b. Riparian vegetation communities of the American Pacific Northwest are tied to multi-scale environmental filters. *River Research and Applications*. DOI: 10.1002/rra.2815

Johnson SL, Rodgers JD, Solazzi MF, Nickelson TE. 2005. Effects of an increase in large wood on abundance and survival of juvenile salmonids. *Oncorhynchus* spp.. in an Oregon coastal stream. *Canadian Journal of Fisheries and Aquatic Sciences* **62***:* 412–424.

Kasprak A, Magilligan FJ, Nislow KH, Snyder NP. 2012. A LiDAR-derived evaluation of watershed-scale large woody debris sources and recruitment mechanisms*:* coastal Maine, USA. *River Research and Applications* **28**: 1462–1476.

Liaw A, Wiener M. 2002. Classification and Regression by randomForest. *R News* **2***:* 18–22.

Macdonald DW, Tattersall FH, Brown ED, Balharry D. 1995. Reintroducing the European Beaver to Britain*:* nostalgic meddling or restoring biodiversity? *Mammal Review* **25***:* 161–200.

Magilligan FJ, Nislow KH, Fisher GB, Wright J, Mackey G, Laser M. 2008. The geomorphic function and characteristics of large woody debris in low gradient rivers, coastal Maine, USA. *Geomorphology* **97***:* 467–482.

Malanson GP, Butler DR. 1990. Woody Debris, Sediment, and Riparian Vegetation of a Subalpine River, Montana, U.S.A. *Arctic and Alpine Research* **22**: 183–194.

Manners RB, Doyle MW, Small MJ. 2007. Structure and hydraulics of natural woody debris jams. *Water Resources Research* **43**: 6.

Martin DJ, Benda LE. 2001. Patterns of Instream Wood Recruitment and Transport at the Watershed Scale. *Transactions of the American Fisheries Society* **130**: 940–958.

Hervé, M. 2015. RVAideMemoire*:* Diverse Basic Statistical and Graphical Functions.

May CL, Gresswell RE. 2003. Processes and rates of sediment and wood accumulation in headwater streams of the Oregon Coast Range, USA. *Earth Surface Processes and Landforms* **28***:* 409–424.

Meredith C, Roper B, Archer E. 2014. Reductions in Instream Wood in Streams near Roads in the Interior Columbia River Basin. *North American Journal of Fisheries Management* **34**: 493–506.

Miller TL using F code by A. 2009. leaps: regression subset selection.

Montgomery DR. 1999. Process domains and the river continuum. *Journal of the American Water Resources Association* **35**: 397–410.

Montgomery DR, Collins BD, Buffington JM, Abbe TB. 2003. Geomorphic effects of wood in rivers. Gregory, Stan V.; Boyer, Kathryn L.; Gurnell, Angela M., eds. The ecology and management of wood in world rivers. American Fisheries Society Symposium, pp 21–47

Nehlsen W. 1997. Prioritizing Watersheds in Oregon for Salmon Restoration. *Restoration Ecology* **5**: 25–33.

Peck DV, Lazorchak JM, Klemm DJ. 2002. Environmental Monitoring and Assessment Program–surface Waters: Western Pilot Study Field Operations Manual for Wadeable Streams. National Health and Environmental Effects Research Laboratory [and] National Exposure Research Laboratory, Office of Research and Development, US Environmental Protection Agency

Polvi L, Wohl E. 2013. Biotic Drivers of Stream Planform: Implications for Understanding the Past and Restoring the Future. *BioScience* **63**: 439–452.

Polvi LE, Wohl EE, Merritt DM. 2011. Geomorphic and process domain controls on riparian zones in the Colorado Front Range. *Geomorphology* **125**: 504–516.

PRISM Climate Group. 2012. PRISM Climate Data.

R Core Team. 2014. R: A Language and Environment for Statistical Computing. R Foundation for Statistical Computing, Vienna, Austria

Ralph SC, Poole GC, Conquest LL, Naiman RJ. 1994. Stream Channel Morphology and Woody Debris in Logged and Unlogged Basins of Western Washington. *Canadian Journal of Fisheries and Aquatic Sciences* **51**: 37–51.

Sarr DA, Hibbs DE, Shatford JPA, Momsen R. 2011. Influences of life history, environmental gradients, and disturbance on riparian tree regeneration in Western Oregon. *Forest Ecology and Management* **261**: 1241–1253.

Thompson DM. 1995. The effects of large organic debris on sediment processes and stream morphology in Vermont. *Geomorphology* **11**: 235–244.

USEPA. US Environmental Protection Agency. . 2006. Wadeable Streams Assessment: a collaborative survey of the Nation's streams. EPA/841/B-06/002. US Environmental Protection Agency Washington, DC

Walter RC, Merritts DJ. 2008. Natural Streams and the Legacy of Water-Powered Mills. *Science* **319***:* 299–304.

Wohl E. 2014. A legacy of absence*:* Wood removal in US rivers. *Progress in Physical Geography* **38***:* 637–663.

Wohl E, Beckman N. 2014. Controls on the longitudinal distribution of channel-spanning logjams in the Colorado Front Range, USA. *River Research and Applications* **30***:* 112–131.

Figures

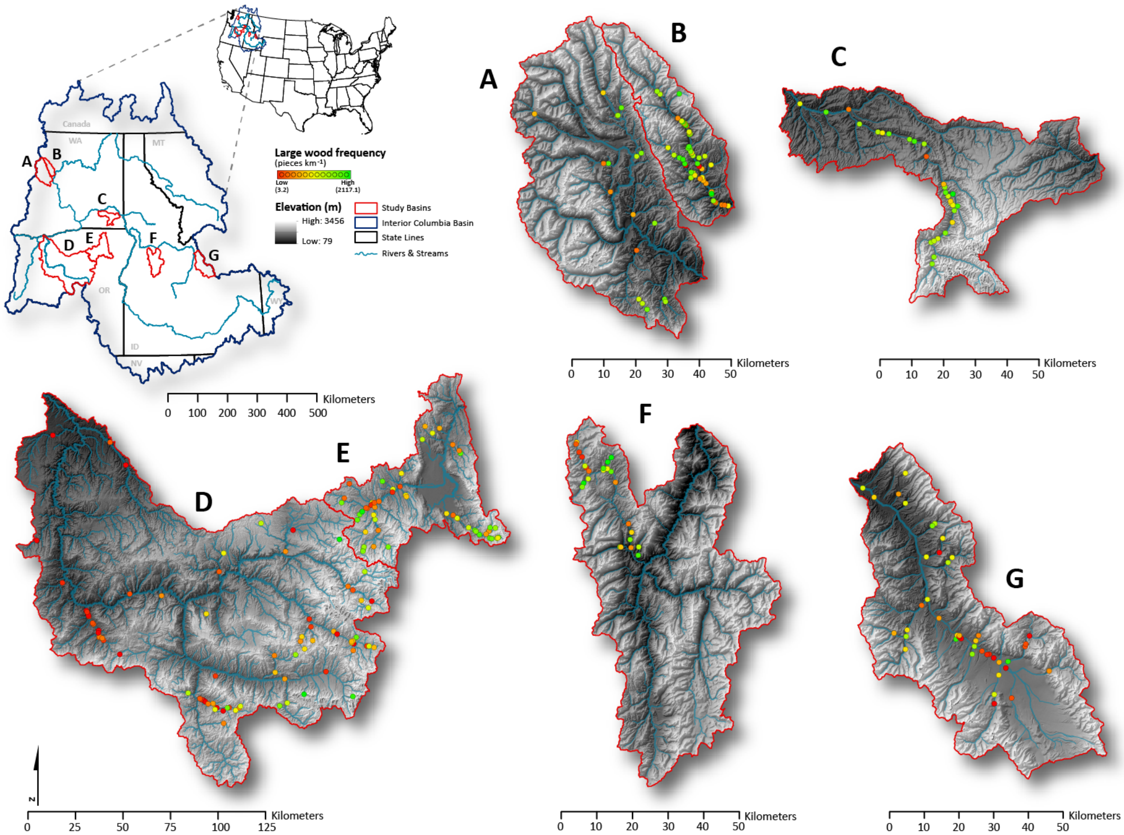

Figure 1. Map of study sub-basins within the larger Columbia River Basin, USA: the Wenatchee (A), Entiat (B), Tucannon (C), John Day (D), Grande Ronde (E), Lemhi (F), and South Fork Salmon (G).

PeerJ PrePrints | https://dx.doi.org/10.7287/peerj.preprints.1256v1 | CC-BY 4.0 Open Access | rec: 21 Jul 2015, publ: 21 Jul 2015

Figure 2. Representative reaches within sub-basins of the Columbia River Basin, USA. Sub-basin photos from top to bottom: Wenatchee, Entiat, Tucannon, John Day, Grande Ronde, Lemhi, and South Fork Salmon. Sub-basin outlines correspond to letters A-G in figure one.

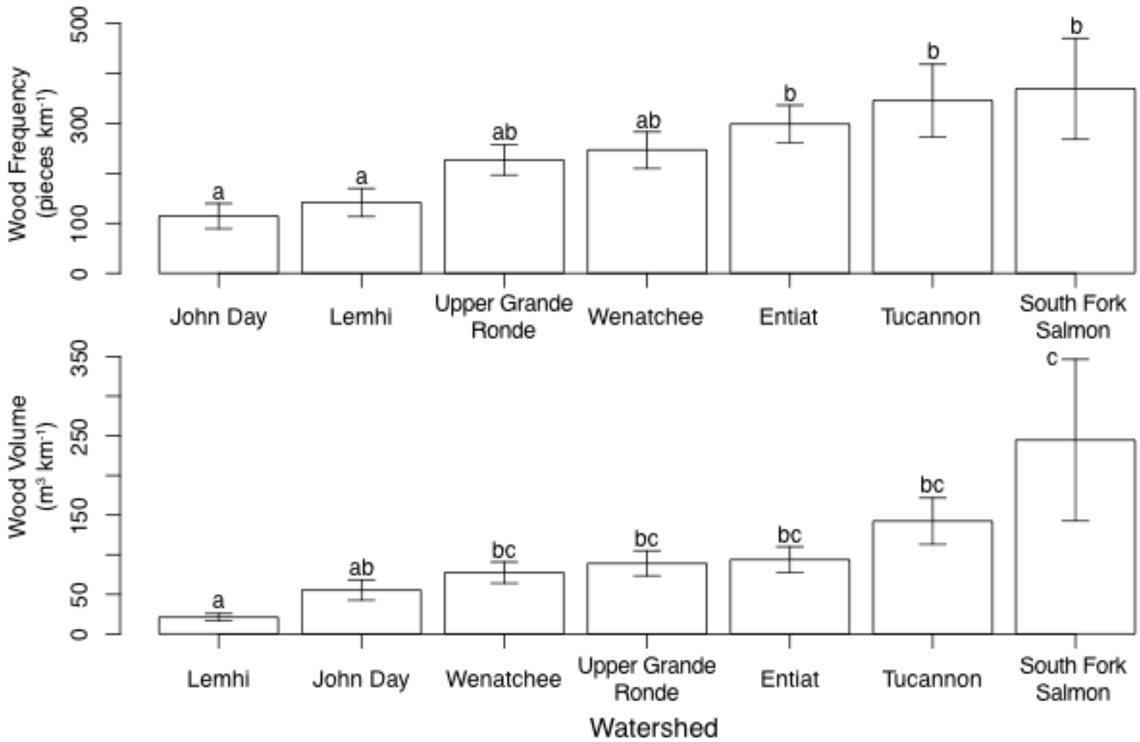

Figure 3. Mean large wood frequency and volume by sub-basin. Letters indicate pairwise differences between groups calculated from permutational t-tests with Bonferroni corrected *P*-values. Error bars are ± standard error of the mean.

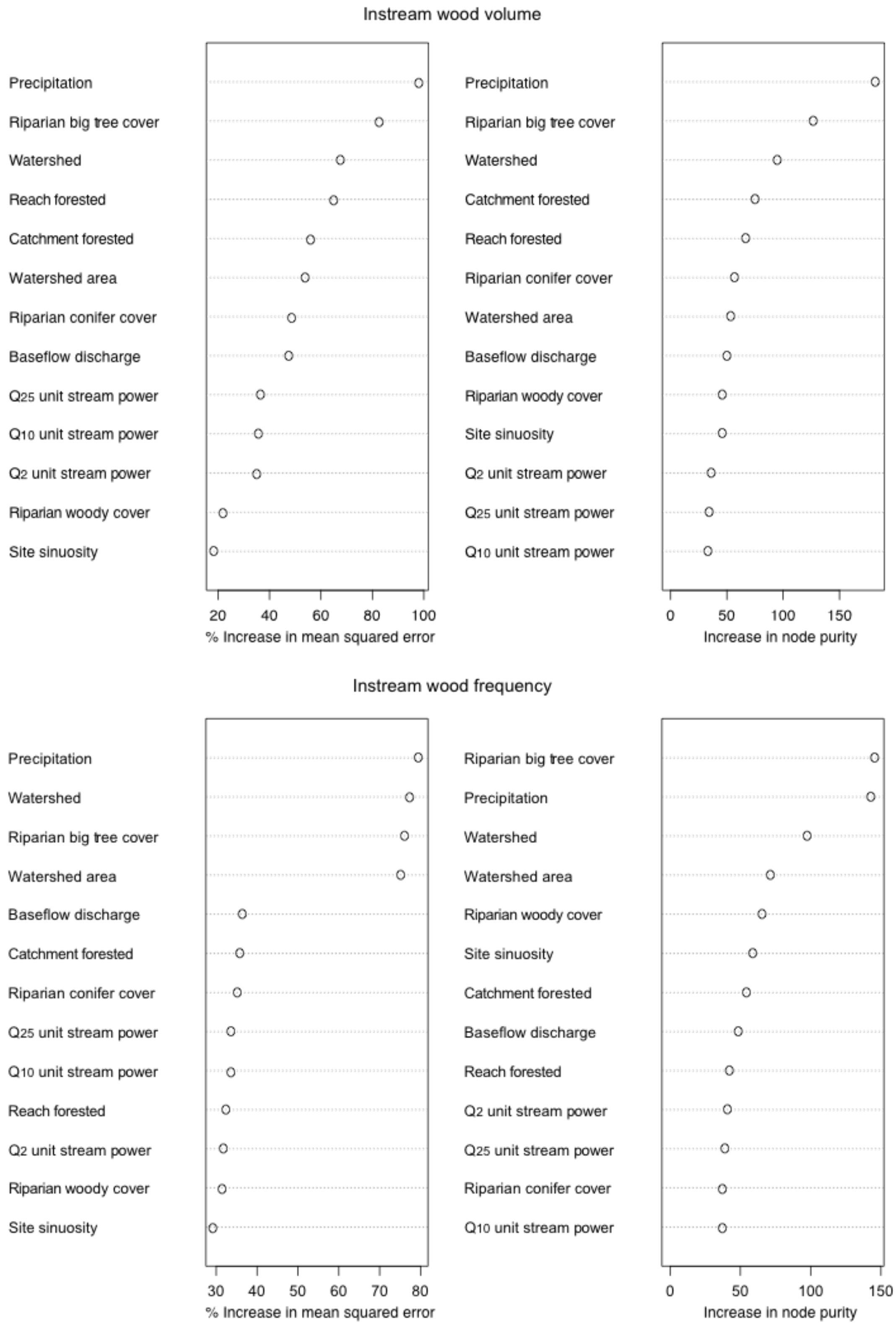

Figure 4. Variable importance plots from random forest models for wood volume and frequency across all seven sub-basins within the Columbia River Basin. Precipitation, riparian

big tree cover, and watershed were the three most important predictors of wood volume and frequency.

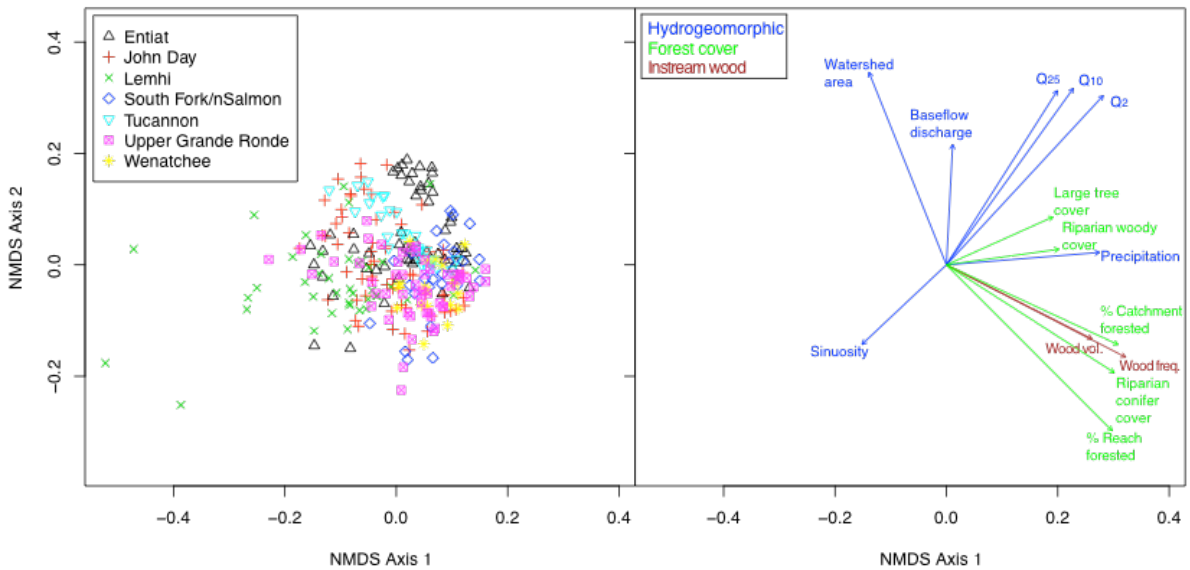

Figure 5. Non-metric multidimensional scaling ordination of log-transformed hydrologic and riparian forest variables at individual sample reaches (left) and multiple regression model fits of individual hydrologic (blue), riparian forest (green), and wood (brown) variables to the ordination space. Wood metrics were not used in calculating multivariate space between reaches and are fit for illustration.

Tables

Table 1. A summary of explanatory reach and catchment hydrologic, physical, and vegetation variables by study watershed. Means are presented with standard deviations in parentheses.

	Watershed characteristics											
				Unit stream power								
Watershed	Site sinuosity	Precipi-tation	Water-shed area	Q_2	Q_{10}	Q_{25}	Base flow dis-charge	Catch-ment forest cover	Reach forest cover	Riparian conifer cover	Riparian woody cover	Big tree cover
Entiat (n = 57)	1.19 (0.22)	1.08 (0.19)	462.84 (336.16)	25223 (16306)	47026 (30380)	57811 (37388)	3.20 (2.75)	66.06 (14.83)	18.42 (21.62)	4.56 (5.80)	67.13 (25.33)	9.28 (8.35)
John Day (n = 75)	1.20 (0.20)	0.54 (0.13)	238.96 (301.59)	15460 (11051)	42328 (34055)	58975 (48265)	0.14 (0.22)	71.95 (24.55)	30.66 (26.77)	4.07 (5.52)	46.46 (24.61)	3.76 (4.64)
Lemhi (n = 43)	1.32 (0.28)	0.54 (0.14)	502.04 (806.69)	12658 (18132)	25760 (34929)	32610 (43490)	0.53 (0.72)	41.69 (20.34)	23.10 (20.06)	0.83 (2.19)	53.82 (29.90)	2.91 (5.05)
South Fork Salmon (n = 25)	1.33 (0.28)	1.24 (0.13)	141.84 (163.10)	40855 (33333)	51896 (41188)	56266 (44331)	1.30 (0.83)	80.18 (11.32)	57.08 (15.50)	6.36 (5.36)	53.84 (26.03)	5.43 (4.10)
Tucannon (n = 28)	1.16 (0.12)	0.97 (0.16)	348.41 (270.13)	33008 (15880)	35422 (11769)	43958 (14336)	1.59 (0.63)	70.85 (20.97)	22.09 (20.09)	2.10 (3.05)	60.31 (31.38)	8.43 (6.38)
Upper Grande Ronde (n = 54)	1.20 (0.25)	0.84 (0.20)	166.62 (230.23)	17065 (11452)	29908 (18511)	35693 (21523)	0.20 (0.22)	80.10 (6.42)	38.06 (24.15)	7.59 (5.93)	53.76 (28.02)	7.81 (6.09)
Wenatchee (n = 18)	1.18 (0.17)	1.23 (0.49)	97.37 (128.05)	15460 (11051)	42328 (34055)	58975 (48265)	0.77 (0.80)	80.34 (6.15)	44.66 (19.81)	8.94 (7.58)	84.68 (26.49)	7.91 (6.81)

Table 2. Summary of measured field variables and data sources

Variable	Data Source	Description
Large wood frequency (pieces km^{-1})	Field measured	Instream wood frequency measured during site visits and scaled to pieces/river kilometer.
Large wood volume (m^3 km^{-1})	Field measured	Instream wood volume measured during site visits and scaled to pieces/river kilometer
Site sinuosity (%)	Field measured	Measured as the proportion of
Watershed area (km^2)	GIS- derived	Total watershed area upslope of the bottom of the sample reach.
Precipitation (m)	GIS- derived	Mean precipitation within the watershed area upslope of the bottom of the sampled reach.
Q_2 unit stream power (Watts m^{-2})	Calculated from field data	Calculated using USGS regional curves for stream discharge.
Q_{10} unit stream power (Watts m^{-2})	Calculated from field data	Calculated using USGS regional curves for stream discharge.
Q_{25} unit stream power (Watts m^{-2})	Calculated from field data	Calculated using USGS regional curves for stream discharge.
Site base flow discharge (m^3 S^{-1})	Field measured	Measured at a cross-section within each reach using standard depth-velocity relationships.
Catchment forest cover (%)	GIS-derived	Calculated using LANDFIRE data and national elevation datasets. LANDFIRE forest vegetation was calculated as a percentage for the area upslope of the bottom of each sampled reach.
Reach forest cover (%)	GIS-derived	Calculated using LANDFIRE data and national elevation datasets within a 30m buffer of the sampled reach.
Riparian conifer cover (%)	Field measured	Measured onsite within ten 10 x 10 m^2 vegetation plots and averaged to yield a reach level average. Includes any coniferous overstory tree.
Riparian woody cover (%)	Field measured	Measured onsite within ten 10 x 10 m^2 vegetation plots and averaged to yield a reach level average. Includes all shrub canopy and overstory woody

		vegetation cover.
Big tree cover (%)	Field measured	Measured onsite within ten 10 x 10 m^2 vegetation plots and averaged to yield a reach level average. Large trees include any overstory tree >0.3m in diameter at breast height.
Water surface gradient (%)	Field measured	Measured onsite using total station surveys and validated from digital elevation models
Bankfull width (m)	Field measured	Measured onsite at five cross-sections using standard stick and tape methods

Table 3. Variables included in final regression models (coefficients in parentheses) for large wood volume and frequency for each sub-basin. Models were constructed from subsets of hydrogeomorphic and riparian forest cover variables to represent both hydrologic and ecological processes while excluding sets of correlated variables from models ($R^2 > 0.6$). All models were selected from candidate models based on exhaustive model selection criteria using the "regsubsets" function in the leaps R package. Models were selected based on BIC and Δ BIC.

Sub-basin	Model	Adj. R^2	BIC	Δ BIC	Final watershed models
Entiat	Volume	0.07	2.8	0	Precipitation (+)
		0.11	3.4	0.6	Precipitation (+), Watershed Area (-)
		0.12	5.7	2.9	Precipitation (+), Watershed Area (-), Riparian conifer cover (-)
	Freq.	0.09	4.5	0	Reach forest cover (+), Riparian conifer cover (-)
		0.02	5.6	1.1	Watershed Area (-)
		0.09	7.4	2.9	Precipitation (+), Reach forest cover (+), Riparian conifer cover (-)
John Day	Volume	0.59	-46.9	0	Reach forest cover (+), Big tree cover (+)
		0.60	-45.1	1.8	Watershed Area (-), Reach forest cover (+), Big tree cover (+)
		0.55	-44.3	2.6	Reach forest cover (+)
	Freq.	0.44	-23.7	0	Watershed Area (-), Reach forest cover (+), Big tree cover (+)
		0.45	-21.9	1.8	Watershed Area (-), Reach forest cover (+), Riparian woody cover (+), Big tree cover (+)
		0.39	-21.5	2.2	Reach forest cover (+), Big tree cover (+)
Lemhi	Volume	0.38	-11.0	0	Watershed Area (+), Catchment forest cover (+)
		0.37	-8.3	2.7	Watershed Area (+), Q25 Unit stream power (+), Catchment forest cover (+)
		0.18	-2.0	9	Watershed Area (+), Q25 Unit stream power (+), Catchment forest cover (+), Big tree cover (+)
	Freq.	0.31	-6.7	0	Watershed Area (+), Catchment forest cover (+)
		0.33	-5.5	1.2	Watershed Area (+), Q25 Unit stream power (+), Catchment forest cover (+)
		0.22	-4.5	2.2	Catchment forest cover (+)
South Fork Salmon	Volume	0.35	0.7	0	Baseflow discharge (-), Reach forest cover (+), Riparian woody cover (-), Big tree cover (+)
		0.15	1.2	0.5	Baseflow discharge (-)

		0.21	1.5	0.8	Baseflow discharge (-), Riparian woody cover (-)
	Freq.	0.30	-1.4	0	Baseflow discharge (-), Riparian woody cover (-)
		0.34	-1.0	0.4	Baseflow discharge (-), Reach forest cover (+), Riparian woody cover (-)
		0.20	-0.3	1.1	Baseflow discharge (-)
Tucannon	Volume	0.43	-7.7	0	Catchment forest cover (+), Big tree cover (-)
		0.37	-7.3	0.4	Catchment forest cover (+)
		0.44	-6.3	1.4	Site sinuosity (+), Catchment forest cover (+), Big tree cover (-)
	Freq.	0.20	1.7	0	Site sinuosity (+), Q25 Unit stream power (+)
		0.13	1.8	0.1	Site sinuosity (+)
		0.22	3	1.3	Site sinuosity (+), Q25 Unit stream power (+), Riparian woody cover (+)
Upper Grande Ronde	Volume	0.26	-3.4	0	Watershed Area (-), Baseflow discharge (+), Reach forest cover (+)
		0.22	-3.3	0.1	Watershed Area (-), Baseflow discharge (+)
		0.26	-0.7	2.7	Precipitation (-), Watershed Area (-), Baseflow discharge (+), Reach forest cover (+)
	Freq.	0.44	-21.6	0	Watershed Area (-), Catchment forest cover (+)
		0.47	-21.5	0.1	Watershed Area (-), Catchment forest cover (+), Riparian conifer cover (+)
		0.49	-20.5	1.1	Watershed Area (-), Catchment forest cover (+), Baseflow discharge (+), Riparian conifer cover (+)
Wenatchee	Volume	0.45	-2.7	0	Precipitation (+), Baseflow discharge (-), Riparian conifer cover (+)
		0.49	-2.4	0.3	Precipitation (+), Q25 Unit stream power (+), Baseflow discharge (-), Riparian conifer cover (+)
		0.38	-2.2	0.5	Q25 Unit stream power (+), Riparian conifer cover (+)
	Freq.	0.54	-6	0	Watershed Area (-), Riparian woody cover (+), Big tree cover (+)
		0.54	-4.2	1.8	Watershed Area (-), Baseflow discharge (-), Riparian woody cover (+), Big tree cover (+)
		0.44	-4.2	1.8	Watershed Area (-), Riparian woody cover (+),

6

Supplemental Materials

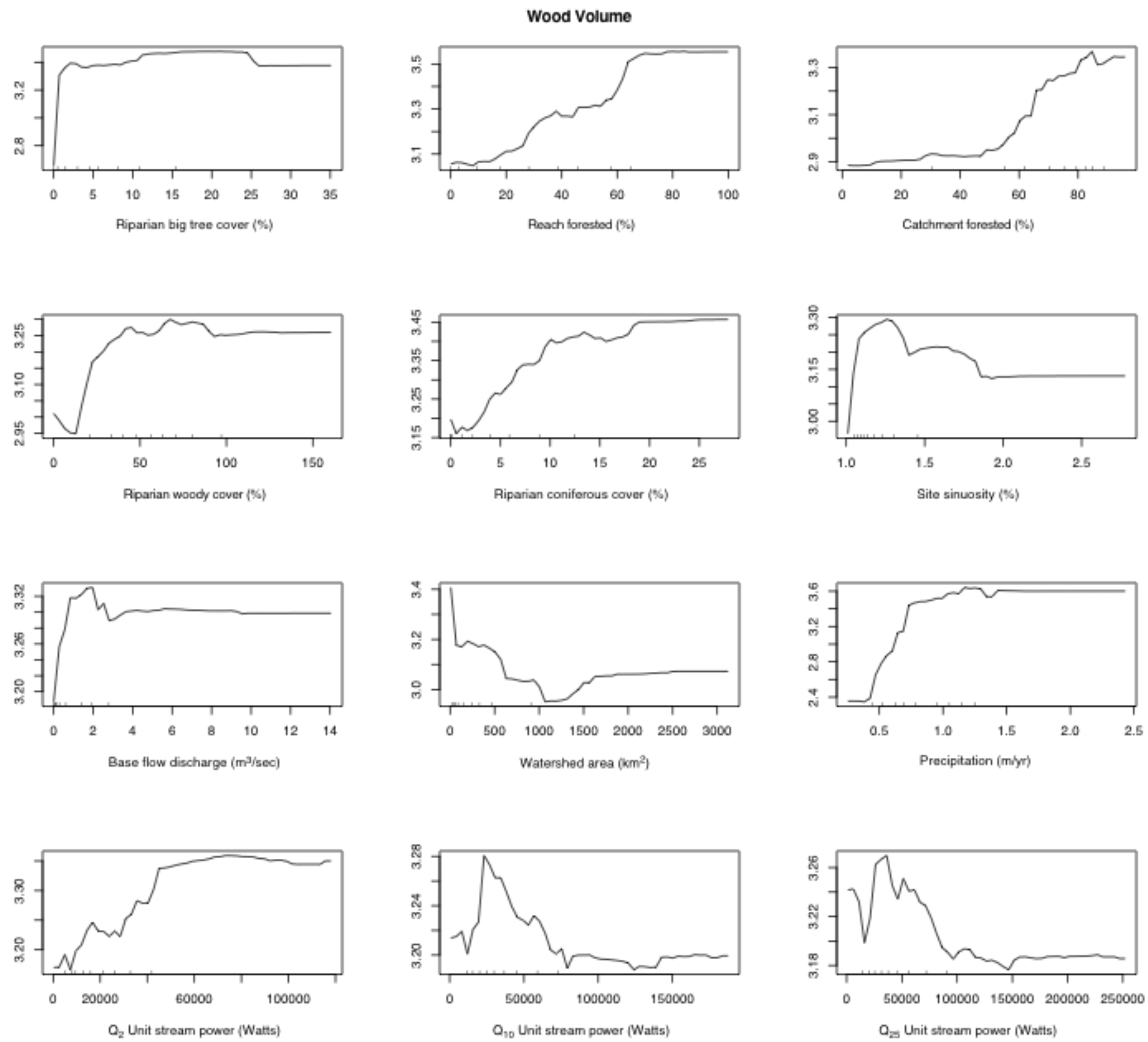

Figure S1. Random forest variable partial dependence plots for log+1 transformed wood volume

PeerJ PrePrints | https://dx.doi.org/10.7287/peerj.preprints.1256v1 | CC-BY 4.0 Open Access | rec: 21 Jul 2015, publ: 21 Jul 2015

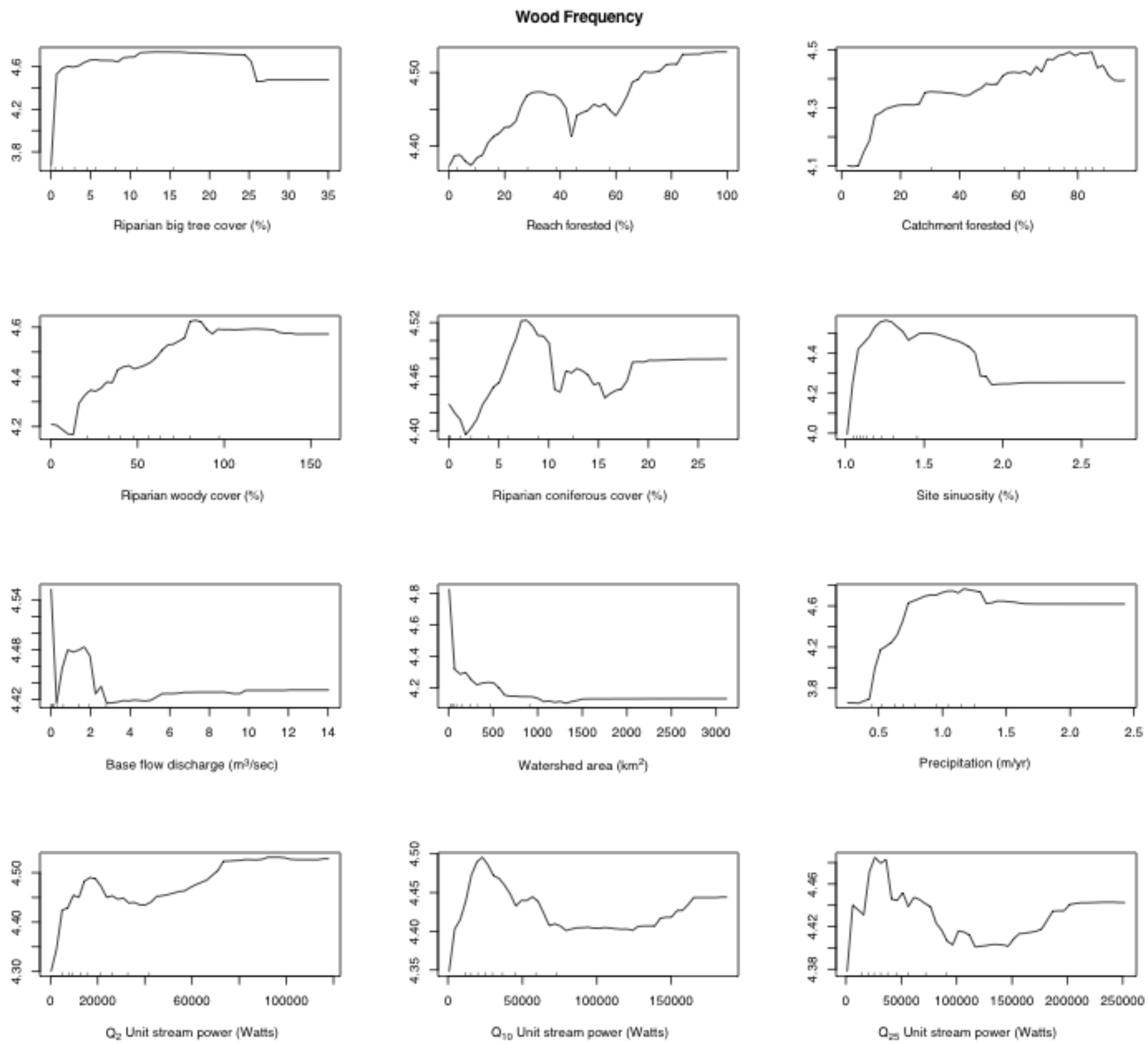

Figure S2. Random forest variable partial dependence plots for log+1 transformed wood frequency.

Table S1: USGS Regional curves used to calculate discharge. Unit stream power calculations that use these equations' discharge outputs are described in the methods in the text.

Watershed	Q	Stream discharge rating relationship equations	Source
Entiat	Q2	$= 0.25 * (DA)^{0.880} * (P)^{1.7}$	(Sumioka et al. 1998)
	Q10	$= 0.179 * (DA)^{0.856} * (P)^{1.37}$	
	Q25	$= 0.341 * (DA)^{0.850} * (P)^{1.26}$	
John Day	Q2	$= 13.1\ (DA)^{0.713}$	(Thomas et al. 1995)
	Q10	$= 55.7\ (DA)^{0.727} * (WE/1{,}000)^{-0.353}$	
	Q25	$= 84.7\ (DA)^{0.727} * (WE/1{,}000)^{-0.438}$	
Lemhi	Q2	$= 0.000258\ (DA)^{0.893} * (P)^{3.15}$	(Berenbrock 2002)
	Q10	$= 0.00632\ (DA)^{0.824} * (P)^{2.45}$	
	Q25	$= 0.0181\ (DA)^{0.801} * (P)^{2.22}$	
South Fork Salmon	Q2	$= 0.0297\ (DA)^{0.995} *(P)^{2.20}\ (NF30+1)^{-0.664}$	(Berenbrock 2002)
	Q10	$= 0.178\ (DA)^{0.957} * (P)^{1.79}\ (NF30+1)^{-0.571}$	
	Q25	$= 0.319\ (DA)^{0.943} * (P)^{1.66}\ (NF30+1)^{-0.538}$	
Tucannon	Q2	$= 0.803(DA)^{0.672} * (P)^{1.16}$	(Sumioka et al. 1998)
	Q10	$= 15.4(DA)^{0.597} * (P)^{0.662}$	
	Q25	$= 41.1(DA)^{0.570} * (P)^{0.508}$	
Upper Grande Ronde	Q2	$= 0.508\ (WA)^{0.82} * (P)^{1.36}\ (1+F)^{-0.27}$	(Jennings et al. 1994)
	Q10	$= 5.28\ (WA)^{0.78} * (P)^{0.96}\ (1+F)^{-0.32}$	
	Q25	$= 11.8\ (WA)^{0.77} * (P)^{0.83}\ (1+F)^{-0.35}$	
Wenatchee	Q2	$Q=.0.25 * (DA)^{0.880} * (P)^{1.7}$	(Sumioka et al. 1998)
	Q10	$Q=.179 * (DA)^{0.856} * (P)^{1.37}$	
	Q25	$Q=.341 * (DA)^{0.850} * (P)^{1.26}$	